厚生労働科学研究費補助金

新型インフルエンザ等新興・再興感染症研究事業

エンベロープウイルス粒子形成の分子基盤の解明と創薬に向けた研究開発

平成２４年度　総括研究報告書

研究代表者　森田　英嗣

目　　次

厚生労働科学研究費補助金（新型インフルエンザ等新興・再興感染症研究事業）

I. 総括研究報告書

エンベロープウイルス粒子形成の分子基盤の解明と創薬に向けた研究開発に関する研究

研究代表者　森田　英嗣　大阪大学微生物病研究所　特任准教授

研究要旨

エンベロープウイルスは、ウイルス遺伝子を内包したコア蛋白質が、宿主細胞の生体膜を通過することによって外被膜 (エンベロープ) を獲得し感染性粒子となる。この過程には様々な宿主因子が関与することから、その分子機構解明によって創薬に繋がる知見が得られると期待される。本研究課題はデングウイルスとインフルエンザウイルスの２種のエンベロープウイルスに焦点を当てており、平成２４年度はデングウイルスの解析を先行してきた。デングウイルスは、感染後期過程に宿主細胞内膜系を大規模に再構築し、ウイルス複製オルガネラと呼ばれる膜に囲まれた構造物を形成する。小胞体 (ER) 近傍に形成されるこの複製オルガネラには、ウイルスゲノム複製の場として、ウイルス蛋白質に加え、多くの宿主因子が集積すると考えられている。本研究では、複製オルガネラ形成に関与する宿主因子を同定することを目的とし、ウイルス感染細胞から精製した複製オルガネラに対して、SILAC 法及び IP-MS 法による網羅的プロテオミクス解析を行い、ウイルス感染細胞特異的に複製オルガネラ画分にリクルートされる宿主因子群を多数同定した。その中には複数の ESCRT (endosomal sorting complex required for transport) 因子が含まれていた。ウイルス複製における ESCRT 因子群の役割を明らかにするために、種々のドミナントネガティブ変異体発現及び siRNA によるノックダウンの影響を調べたところ TSG101、CHMP2、CHMP3、CHMP4 がウイルス複製に関与することが示された。これらの結果は、ESCRT 経路が、フラビウイルス複製において重要な役割を担っていることを示している。また、LC3 等の複数のオートファジー関連因子が複製オルガネラに集積することが見出された。オートファジー形成に関与する FIP200 及び p62 の遺伝子欠損細胞では、ウイルス増殖が著しく阻害されていることが明らかとなった。この結果は、宿主オートファジーに作用する因子がウイルス増殖に関与することを示している。これらの解析は、未だ治療法が確立されていないデングウイルス感染症克服の為の新規薬剤開発につながるものと期待される。

A．研究目的

近年、インフルエンザウイルス感染症において、既存のノイラミニダーゼ阻害剤に対する耐性株出現に関する様々な報告がなされ、新たな分子標的薬の開発が求められている。また、デングウイルスにおいては、毎年世界で１億人の感染者がいるにもかかわらず、未だ有効な治療法がなく、抗ウイルス薬の開発が求められている。本研究は、インフルエンザウイルス及び、海外からの流入感染症として警戒が必要とされているデングウイルスの２種類のエンベロープウイルスに着目し、細胞内での複製機構の解明と新規抗ウイルス薬開発のための分子基盤の確立を目的としている。

インフルエンザウイルス及びデングウイルスは共にエンベロープウイルスに属し、感染後期過程においてウイルス遺伝子を内包したコア蛋白質が、宿主細胞の生体膜を通過することによってエンベロープを獲得し細胞外に放出される。これまでのレトロウイルスやラブドウイルスなどの、他のエンベロープウイルスの解析から、外被膜獲得のプロセスに ESCRT (endosomal sorting complex required for transport)と呼ばれる宿主側因子が共通に関与していることが示された。しかしながら、インフルエンザウイルスやデングウイルスに関しては、ESCRT の関与を含め、その分子機構は未だ不明である。

本研究では、これら２種のエンベロープウイルスの粒子形成機構を明らかにするために、ま

ず、各種ウイルス因子に結合する蛋白質及びウイルス複製オルガネラに対する網羅的なプロテオミクス解析を行い、ウイルス増殖に必要な宿主因子の検索を行った。これら解析によって得られた候補因子群に対して、遺伝子のクローニングを行い、各種細胞生物学的及び生化学的な解析を行い、その作用機序解明を試みた。

B．研究方法

デングウイルスに代表されるフラビウイルスは、感染すると宿主細胞の小胞体近傍に複製オルガネラと呼ばれる新たな構造物を形成する。本研究では、デングウイルス感染 Huh7 細胞を破砕した後、ショ糖密度勾配遠心分離法により、ウイルス複製オルガネラ陽性画分を精製し、SILAC (Stable isotope labeling with amino acids in cell culture) 法による定量プロテオミクス解析にて、感染特異的に複製オルガネラへリクルートされる宿主因子を同定した。また、各種ウイルス蛋白質に対してアフィニティーキャプチャーMS (Mass Spectrometry) 解析を行い、ウイルス蛋白質に結合する宿主蛋白質因子を網羅的に同定した (図１)。

2 型デングウイルスの標準株である NGC (New Guinea C) 株は、トランスフェクション効率の高い 293T 細胞に対して高い増殖性を示さない。そこで、本研究では、長期培養により NGC 株の 293T 細胞へのアダプテーションを行った。このアダプテーションさせた 2 型デングウイルス株と、同科フラビウイルスである日本脳炎ウイルス(Japanese encephalitis virus: JEV)を用いて、293T 細胞における各種宿主因子のフラビウイルス増殖に対する影響を検討した。

前述のプロテオミクス解析によって同定された候補遺伝子群に対して、個別の遺伝子クローニングを行い、既知の情報をもとに各種ドミナントネガティブ変異体を作成し、その発現によってウイルス増殖がどのように変化するのか検討した。また、各種候補因子がウイルス感染細胞の何処に局在するのか、間接免疫蛍光染色法によって解析した。また、siRNA による遺伝子ノックダウンを行い、候補因子のウイルス増殖における重要性を解析した (図１)。

（倫理面への配慮）

遺伝子操作に関しては、大阪大学微生物病研究所の遺伝子組換え実験委員会の審査を受け承認されている。また、微生物やウイルスの使用に関しては、バイオセーフティ委員会の審査を受け了承されている。

C．研究結果

１、プロテオミクス解析による宿主因子の同定

デングウイルス感染 Huh7 細胞より複製複合体画分を精製し、SILAC 法による定量プロテオミクス解析を、非感染細胞より精製した画分を対照に用いて行ったところ、1941 種類の宿主因子に対して蛋白質の同定と比較定量を行うことに成功した。この定量プロテオミクス解析の結果、PI4KIII-α や OSBPL8 など既に複製複合体で作用することが報告されている宿主因子が、感染によってウイルス複製複合体にリクルートされる因子として同定された。また、デングウイルスの非構造蛋白質を 293T 細胞に発現させ、アフィニティー精製によって共精製される宿主因子を 430 種類同定した。上記プロテオミクス解析によって同定された因子群の中から、バイオインフォマティクス解析により 120 種類の蛋白質を要解析候補宿主因子として抽出した。そのうち 88 種類の蛋白質をコードする遺伝子の cDNA のクローニングを行い、FLAG タグ付き哺乳動物細胞発現ベクターを作成した。

2 型デングウイルス NGC 株を 293T へ感染させ３ヶ月間に渡り長期培養を行ったところ、感染３日後に 10^7FFU/ml のウイルスを放出する 293T 順応化 NGC 株: DENV2-NGC^{293T} を樹立することに成功した。このウイルス株樹立により初めて、プロテオミクス解析によって同定された候補因子に対して 293T 細胞での解析を行うことが可能となった。DENV2-NGC^{293T} 及び JEV を用いて、プロテオミクス解析によって同定された候補宿主因子群の感染細胞内での局在を観察したところ、10 種類の候補因子がウイルス蛋白質と共局在することが示された。また、ウイルスの増殖における、これら因子群の強発現の影響を調べたところ、7 種類の蛋白質に関して強いウイルス増殖阻害効果(対照に比べ 1/10 以下)が認められた。現在それぞれの候補因子群に対して siRNA による遺伝子ノックダウンを行い、ウイルス増殖における重要性について検討している。

２、ESCRT 経路の関与

一連のプロテオミクス解析により、宿主 ESCRT 因子である CHMP6、CHMP7 が感染特異的に複製オルガネラにリクルートされる因子

として同定された。また、VPS4A と VPS4B が NS3、また CHMP1A と CHMP5 が NS5 と共に免疫沈降法によって共沈することが明らかとなった (図２)。さらに、ウイルス感染細胞内において、種々の ESCRT 因子がウイルス複製オルガネラに局在することが確認された。これらの結果は、宿主 ESCRT 因子群がウイルス因子と細胞内にて相互作用していることを示している。ESCRT 因子群の役割を明らかにするために、種々のドミナントネガティブ変異体発現の影響を調べたところ、CHMP2、CHMP7 以外の全ての ESCRT-III 変異体発現がウイルス増殖を負に制御することが示された (図３)。また、ESCRT 因子群に対する網羅的な siRNA ノックダウンによるスクリーニングを行ったところ、TSG101 および CHMP2、CHMP3、 CHMP4 のノックダウンによりウイルスの増殖が顕著に (対照に比べ 1/100-1/1000 程度) 阻害されることが明らかとなった (図４)。これらの結果は、これまでにエンドソームや原形質膜においてのみ作用すると考えられていた ESCRT 経路が、ER 上でのデングウイルス複製においても重要な役割を担っていることを示している。現在、ウイルス因子と宿主 ESCRT 因子との直接結合の有無について酵母 two ハイブリッド法を用いて検索している。

3、オートファジー経路の関与

ウイルス複製オルガネラの定量プロテオミクス解析より、宿主細胞のオートファゴソームのマーカーである LC3 が感染特異的に複製オルガネラにリクルートされることが示された。デングウイルスを感染させると細胞内においてオートファゴソームマーカーである LC3 の輝点形成が認められた。この結果は、ウイルスが感染すると宿主オートファジーが誘導されることを示している。オートファジーのウイルス増殖への役割を明らかにするために、各種 ATG (*Autophagy*) 関連遺伝子欠損マウス繊維芽細胞 (ATG3-/-、ATG5-/-、ATG7-/-、ATG9L1-/-、ATG14L-/-、FIP200-/-、Beclin-/-、Rubicon-/-、p62-/-) に、JEV を感染させその増殖能を調べたところ、ATG3-/-、ATG5-/-、ATG7-/-、ATG9L1-/-、ATG14L-/-、Beclin-/-、Rubicon-/-細胞では野生型細胞を用いた場合と変化は認められなかった。しかしながら、FIP200-/-および p62-/-細胞を用いた場合では著しいウイルス増殖阻害 (対照に比べ 1/100 以下) が認められた。この結果より、ウイルスの増殖において、FIP200 および p62 が必要であることが示された。しかしながら、オートファジーに重要な役割を持つ ATG3、ATG5、ATG7 などの因子の欠損はウイルス増殖に影響が無かったことから、オートファジー機構そのものはウイルスの増殖には関与していないことが示された。

D．考察

本研究での定量プロテオミクス解析によって既知の因子が同定されたことから、このアプローチによって同定された他の候補因子群の中にも、ウイルスの増殖に重要な機能をもつものが含まれていると考えられる。実際に、各種候補因子の遺伝子をクローニングし、強発現やドミナントネガティブ体の発現などを個別に解析したところ、複数の因子に関してウイルス増殖に対して役割を持っている可能性が示された。今後、これら候補因子群の詳細な解析により、新たな分子標的薬開発のための候補因子が見出されることが期待される。

本研究のプロテオミクス解析によって ESCRT 因子群がウイルス複製オルガネラにリクルートされる因子として同定された。これまでの解析より、ESCRT 因子群はレトロウイルスやラブドウイルスなど、原形質膜上にてアセンブリーし出芽するエンベロープウイルスの粒子形成に関与することがわかっている。ESCRT 因子群がフラビウイルスの複製又は粒子形成に関与しているということは、ESCRT 因子は原形質膜上やエンドソーム膜上だけでなく、小胞体上でも重要な役割を担っていることが示された。この結果から、ESCRT 因子群の機能的多様性と、膜変形における普遍的な役割が存在することが伺える。ESCRT 経路因子群に対する siRNA によるノックダウンの影響を調べたところ、TSG101、CHMP2、CHMP3、CHMP4 にウイルス増殖に対して重要な役割があることが示された。これらの ESCRT 因子の必要性パターンは、レトロウイルスの粒子形成の場合と酷似しており、ESCRT 因子群の作用機序には各種ウイルス間において一定の共通性があると考えられる。また、現在開発が進められている TSG101 とウイルス蛋白質への結合を標的とした抗ウイルス薬が、フラビウイルスへ応用できる可能性が示された。

本研究のプロテオミクス解析によって宿主オートファジー機構がウイルス感染に関与する可

能性が明らかとなった。マウス繊維芽細胞に感染し増殖することが可能なJEVを用いて実験を行ったところ、オートファジー機構に必須な複数の ATG 因子の遺伝子欠損細胞でも、ウイルスの増殖能は野生型細胞と同等であった。この結果は、オートファジー機構そのものはウイルスの増殖に関与していないことを示している。一方、ATG 因子群のなかでも FIP200 や p62 等の遺伝子欠損細胞ではJEVの増殖能が著しく阻害された。この結果から、FIP200 や p62 はオートファジーへの役割とは独立した機能によってウイルス増殖に関与していることを示している。現在、デングウイルスのマウス細胞への順応化を行っており、今後、デングウイルスにおいても JEV と同様なオートファジー又は ATG 遺伝子の必要性を検討する予定である。

E．結論

本研究によって、デングウイルスの増殖に関与する可能性のある候補宿主因子群が同定された。この中には種々の機能未知の遺伝子が多く含まれており、今後の解析により、ウイルス増殖の詳細な分子機構が明らかになると期待される。また、宿主のESCRT因子とATG因子群がウイルスの増殖に関与することが示された。これらの宿主因子ーウイルス因子相互作用を詳細に解析することによって、抗ウイルス薬開発につながる情報を提供できる可能性がある。さらに、宿主因子-ウイルス因子相互作用の構造を明らかにすることにより*in silico*での創薬につながる情報が得られると期待される。

F．健康危険情報：なし

G．研究発表

1. 論文発表

(1) Katoh H, Okamoto T, Fukuhara T, Kambara H, **Morita E,** Mori Y, Kamitani W, Matsuura Y. Japanese Encephalitis Virus Core Protein Inhibits Stress Granule Formation through an Interaction with Caprin-1 and Facilitates Viral Propagation. ***J Virol.*** 2013 Jan;87(1):489-502

(2) **Morita, E.**, Arii J, Christensen D, Votteler J, Sundquist WI. Attenuated protein expression vectors for use in siRNA rescue experiments. ***Biotechniques.*** 2012 Aug;0(0):1-5.

(3) Tripathi, L.P., Kambara, H., Moriishi, K., **Morita, E.,** Abe, T., Mori, Y., Chen, Y.A., Matsuura, Y., Mizuguchi, K. Proteomic analysis of hepatitis C virus (HCV) core protein transfection and host regulator PA28γ knockout in HCV pathogenesis: a network-based study. ***J Proteome Res.*** 2012 Jul 6;11(7):3664-79.

(4) Fukuhara, T., Kambara, H., Shiokawa, M., Ono, C., Katoh, H., **Morita, E.**, Okuzaki, D., Maehara, Y., Koike, K., Matsuura, Y. Expression of microRNA miR-122 facilitates an efficient replication in nonhepatic cells upon infection with hepatitis C virus. ***J Virol.*** 2012 Aug;86(15):7918-33.

(5) **Morita, E.**, Yoshimori, T. Membrane recruitment of LC3 proteins during autophagosome formation. ***Hepatol Res.*** 2012 42:435-441.

(6) **Morita, E.** ESCRT Differential requirements of mammalian ESCRTs in multivesicular body formation, virus budding and cell division. ***FEBS J.*** 2012 279:1399-406.

2. 学会発表等

(1) **森田 英嗣** ESCRT経路を介したRNAエンベロープウイルス粒子形成の分子メカニズム京都大学ウイルス研究所セミナー 京都大学ウイルス研究所 2012.6.27

(2) **Eiji Morita**. Mechanisms of enveloped RNA virus budding and cytokinesis. NEKKEN Seminar. Institute of Tropical Medicine Nagasaki University 2012.7.18

(3) **森田 英嗣** ESCRT経路を介したRNAエンベロープウイルス粒子形成の分子機構 特別講演 第19回トガ・フラビ・ペスチウイルス研究会 2012.11.12

(4) 加藤 大志、岡本 徹、福原 崇介、寒原 裕登、**森田 英嗣**、森 嘉生、神谷 亘、松浦 善治日本脳炎ウイルスコアタンパク質によるStress Granule抑制機構の解析 第60回日本ウイルス学会学術集会 2012.11.13 大阪

H．知的財産権の出願・登録状況

1. 特許取得：なし。

2. 実用新案登録：なし。

ウイルス増殖に関与する宿主因子の検索

一次スクリーニング(プロテオミクス解析)

- SILAC: stable isotope labeling using amino acids in cell culture
  ウイルス感染細胞より抽出した小胞体画分

- ショットガン法によるIP-MS解析
  ベイト蛋白質: DENV Core, NS2A, NS2B, NS3-N, NS3-C, NS4A, NS4B, NS5
  : JEV Core, NS2A, NS2B, NS3-N, NS3-C, NS4A, NS4B, NS5

二次スクリーニング （>120遺伝子）

- 野生型又はドミナントネガティブ変異体発現によるウイルス増殖への影響
- siRNAによるノックダウンのウイルス増殖に対する影響
- 酵母twoハイブリッド法による直接結合の検索
- 免疫蛍光染色法による細胞内局在

図１：ウイルス増殖に関与する宿主因子検索に関する流れ図

SILAC	ESCRT proteins
	CHMP6, CHMP7
IP-MS	
bait	**ESCRT proteins**
JEV_NS3-N	Vps4A, Vps4B
JEV_NS5	CHMP1A, CHMP5

図2：プロテオミクス解析による一次スクリーニングにて同定されたESCRT因子群

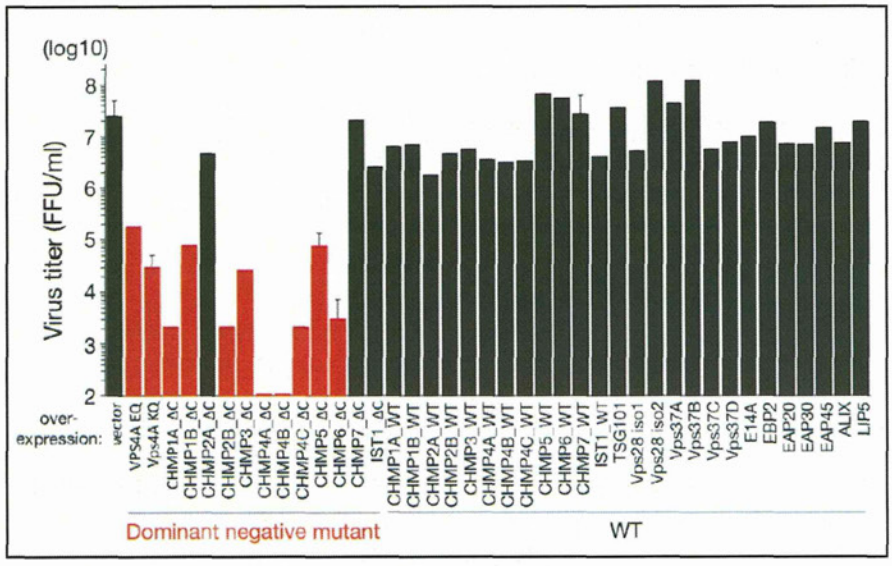

図3：ESCRT因子に対するドミナントネガティブ変異体発現とウイルス増殖に対する影響

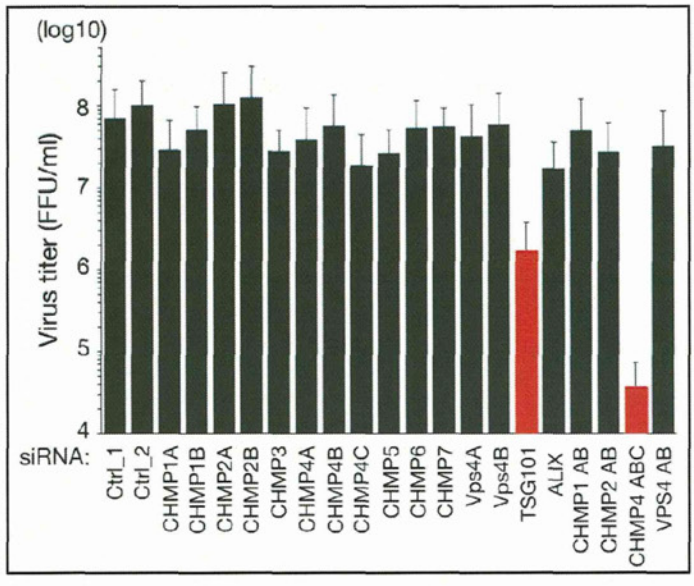

図4： siRNAによるESCRT因子のノックダウンとウイルス増殖に対する影響

II. 研究成果の刊行に関する一覧表

雑誌

発表者氏名	論文タイトル名	発表誌名	巻号	ページ	出版年
Katoh H, Okamoto T, Fukuhara T, Kambara H, **Morita E,** Mori Y, Kamitani W, Matsuura Y.	Japanese Encephalitis Virus Core Protein Inhibits Stress Granule Formation through an Interaction with Caprin-1 and Facilitates Viral Propagation.	***J Virol.***	87(1)	489-502	2013
Morita, E., Arii J, Christensen D, Votteler J, Sundquist WI.	Attenuated protein expression vectors for use in siRNA rescue experiments.	***Biotechniques.***	0	1-5	2012
Tripathi, L.P., Kambara, H., Moriishi, K., **Morita, E.,** Abe, T., Mori, Y., Chen, Y.A., Matsuura, Y., Mizuguchi, K.	Proteomic analysis of hepatitis C virus (HCV) core protein transfection and host regulator PA28γ knockout in HCV pathogenesis: a network-based study.	***J Proteome Res.***	11	3664-3679	2012
Fukuhara, T., Kambara, H., Shiokawa, M., Onoo, C., Katoh, H., **Morita, E.,** Okuzaki, D., Maehara, Y., Koike, K., Matsuura,	Expression of microRNA miR-122 facilitates an efficient replication in nonhepatic cells upon infection with hepatitis C virus.	***J Virol.***	86	7918-7933	2012
Morita, E., Yoshimori, T.	Membrane recruitment of LC3 proteins during autophagosome formation.	***Hepatol Res.***	42	435-441	2012
Morita, E.	ESCRT Differential requirements of mammalian ESCRTs in multivesicular body formation, virus budding and cell division.	***FEBS J.***	279	1399-1406	2012

JVI
Journals.ASM.org

Japanese Encephalitis Virus Core Protein Inhibits Stress Granule Formation through an Interaction with Caprin-1 and Facilitates Viral Propagation

Hiroshi Katoh,[a] Toru Okamoto,[a] Takasuke Fukuhara,[a] Hiroto Kambara,[a] Eiji Morita,[b] Yoshio Mori,[d] Wataru Kamitani,[c] Yoshiharu Matsuura[a]

Department of Molecular Virology,[a] International Research Center for Infectious Diseases,[b] and Global COE Program,[c] Research Institute for Microbial Diseases, Osaka University, Osaka, Japan; Department of Virology III, National Institute of Infectious Diseases, Tokyo, Japan[d]

Stress granules (SGs) are cytoplasmic foci composed of stalled translation preinitiation complexes induced by environmental stress stimuli, including viral infection. Since viral propagation completely depends on the host translational machinery, many viruses have evolved to circumvent the induction of SGs or co-opt SG components. In this study, we found that expression of Japanese encephalitis virus (JEV) core protein inhibits SG formation. Caprin-1 was identified as a binding partner of the core protein by an affinity capture mass spectrometry analysis. Alanine scanning mutagenesis revealed that Lys^{97} and Arg^{98} in the α-helix of the JEV core protein play a crucial role in the interaction with Caprin-1. In cells infected with a mutant JEV in which Lys^{97} and Arg^{98} were replaced with alanines in the core protein, the inhibition of SG formation was abrogated, and viral propagation was impaired. Furthermore, the mutant JEV exhibited attenuated virulence in mice. These results suggest that the JEV core protein circumvents translational shutoff by inhibiting SG formation through an interaction with Caprin-1 and facilitates viral propagation *in vitro* and *in vivo*.

In eukaryotic cells, environmental stresses such as heat shock, oxidative stress, UV irradiation, and viral infection trigger a sudden translational arrest, leading to stress granule (SG) formation (1). SGs are cytoplasmic foci composed of stalled translation preinitiation complexes and are postulated to play a critical role in regulating mRNA metabolism during stress via so-called "mRNA triage" (2). The initiation of SG formation results from phosphorylation of eukaryotic translation initiation factor 2α (eIF2α) at Ser^{51} by various kinases, including protein kinase R (PKR), PKR-like endoplasmic reticulum kinase (PERK), general control nonrepressed 2 (GCN2), and heme-regulated translation inhibitor (HRI), which are commonly activated by double-stranded RNA (dsRNA), endoplasmic reticulum (ER) stress, nutrient starvation, and oxidative stress, respectively. Phosphorylation of eIF2α reduces the amount of eIF2-GTP-tRNA complex and inhibits translation initiation, leading to runoff of elongating ribosomes from mRNA transcripts and the accumulation of stalled translation preinitiation complexes. Thus, SGs are defined by the presence of components of translation initiation machinery, including 40S ribosome subunits, poly(A)-binding protein (PABP), eIF2, eIF3, eIF4A, eIF4E, eIF4G, and eIF5. Then, primary aggregation occurs through several RNA-binding proteins (RBPs), including T-cell intracellular antigen-1 (TIA-1), TIA-1-related protein 1 (TIAR), and Ras-Gap-SH3 domain-binding protein (G3BP). These RBPs are independently self-oligomerized with the stalled initiation factors and with other RBPs, such as USP10, hnRNP Q, cytoplasmic activation/proliferation-associated protein-1 (Caprin-1), and Staufen and with nucleated mRNA-protein complex (mRNP) aggregations (3, 4). SG assembly begins with the simultaneous formation of numerous small mRNP granules which then progressively fuse into larger and fewer structures, a process known as secondary aggregation (5). The aggregation of TIA-1 or TIAR is regulated by molecular chaperones, such as heat shock protein 70 (Hsp70) (3), whereas that of G3BP is controlled by its phosphorylation at Ser^{149} (4). SG formation and disassembly in response to cellular stresses are strictly regulated by multiple factors.

Viral infection can certainly be viewed as a stressor for cells, and SGs have been reported in some virus-infected cells. Since the propagation of viruses is completely reliant on the host translational machinery, stress-induced translational arrest plays an important role in host antiviral defense. To antagonize this host defense, most viruses have evolved to circumvent SG formation during infection. For example, poliovirus (PV) proteinase 3C cleaves G3BP, leading to effective SG dispersion and virus propagation (6). Influenza A virus nonstructural protein 1 (NS1) has been shown to inactivate PKR and prevent SG formation (7). In the case of human immunodeficiency virus 1 (HIV-1) infection, Staufen1 is recruited in ribonucleoproteins for encapsidation through interaction with the Gag protein to prevent SG formation (8). In contrast, some viruses employ alternative mechanisms of translation initiation and promote SG formation to limit cap-dependent translation of host mRNA (9, 10). In addition, vaccinia virus induces cytoplasmic "factories" in which viral translation, replication, and assembly take place. These factories include G3BP and Caprin-1 to promote transcription of viral mRNA (11).

Japanese encephalitis virus (JEV) belongs to the genus *Flavivirus* within the family *Flaviviridae*, which includes other mosquito-borne human pathogens, such as dengue virus (DENV), West Nile virus (WNV), and yellow fever virus, that frequently cause significant morbidity and mortality in mammals and birds (12). JEV has

Received 15 August 2012 Accepted 15 October 2012
Published ahead of print 24 October 2012
Address correspondence to Yoshiharu Matsuura, matsuura@biken.osaka-u.ac.jp.

doi:10.1128/JVI.02186-12

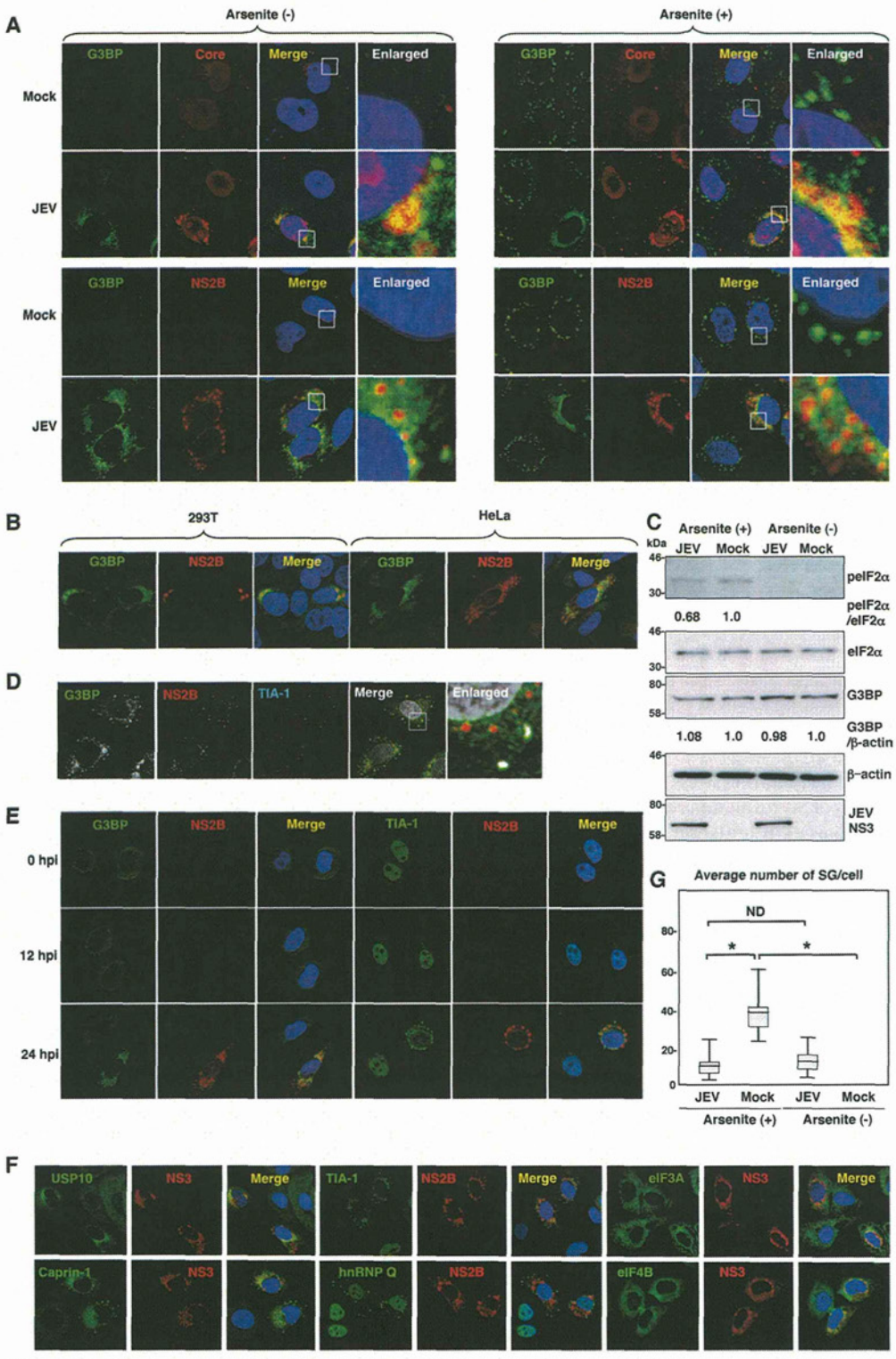

FIG 1 Dynamics of SG-associated factors during JEV infection. (A) Huh7 cells infected with JEV at an MOI of 0.5 were treated with or without 1.0 mM sodium arsenite for 30 min at 37°C, and the levels of expression of G3BP and JEV core protein/NS2B were determined at 24 h postinfection by immunofluorescence analysis with mouse anti-G3BP MAb and rabbit anti-core protein or anti-NS2B PAb, followed by AF488-conjugated anti-mouse IgG (Invitrogen) and AF594-conjugated anti-rabbit IgG, respectively. Cell nuclei were stained with DAPI (blue). (B) Cellular localizations of G3BP and JEV NS2B in 293T and HeLa cells infected with JEV were determined at 24 h postinfection by immunofluorescence analysis with mouse anti-G3BP MAb and rabbit anti-NS2B PAb, followed by AF488-conjugated anti-mouse IgG and AF594-conjugated anti-rabbit IgG, respectively. Cell nuclei were stained with DAPI (blue). (C) Phosphorylation of eIF2α in cells prepared as described in panel A was determined by immunoblotting using the indicated antibodies. The band intensities were quantified by ImageJ

a single-stranded positive-sense RNA genome of approximately 11 kb. The genomic RNA carries a single large open reading frame, and a polyprotein translated from the genome is cleaved co- and posttranslationally by host and viral proteases to yield three structural proteins, the core, precursor membrane (PrM), and envelop (E) proteins, and seven nonstructural (NS) proteins, NS1, NS2A, NS2B, NS3, NS4A, NS4B, and NS5 (13). PrM is further cleaved by the multibasic protease, furin, and matured to membrane (M) protein. The core, M, and E proteins are components of extracellular mature virus particles. NS proteins are not incorporated into particles and are thought to be involved in viral replication, which occurs in close association with ER-derived membranes (14). Previous reports have shown that WNV and DENV inhibit SG formation by sequestering TIA-1 and TIAR through specific interaction with viral RNA (15, 16). In addition, the membrane structure induced by WNV infection was suggested to prevent PKR activation and avoid induction of SG formation (17). In this study, we show that JEV core protein plays an important role in inhibition of SG formation. JEV core protein recruited several SG-associated proteins, including G3BP and USP10, through an interaction with Caprin-1 and suppressed SG formation. Furthermore, a mutant JEV carrying a core protein incapable of binding to Caprin-1 exhibited lower propagation *in vitro* and lower pathogenicity in mice than the wild-type (WT) JEV, suggesting that inhibition of SG formation by the core protein is crucial to antagonize host defense. These results reveal a novel strategy of JEV to inhibit SG formation through an interaction with Caprin-1 and facilitate viral propagation.

MATERIALS AND METHODS

Plasmids. Plasmids encoding FLAG-tagged JEV core protein (pCAGPM-FLAG-Core) and hemagglutinin (HA)-tagged JEV proteins (pCAGPM-HA-JEV proteins) were generated as previously described (18, 19). The cDNA of the core protein of JEV AT31 (amino acid residues 2 to 105) was amplified from the pCAGPM-FLAG-Core plasmid by PCR and cloned into pET21b (Novagen-Merck, Darmstadt, Germany) for expression in bacteria as a His-tagged protein and in pCAG-MCS2-FOS for expression in mammalian cells as a FLAG-One-STrEP (FOS)-tagged protein. The resulting plasmids were designated pET21b-Core-His and pCAG-Core-FOS, respectively. The cDNA of the core protein of DENV2 (amino acid residues 2 to 100) was amplified from the pCAG/FLAG-DEN2C-HA plasmid (19) by PCR and cloned into pCAGPM-N-FLAG. The cDNA of human Caprin-1 was amplified from 293T cells by reverse transcription-PCR (RT-PCR) and cloned into pCAGPM-N-HA (20) and pGEX 6P-1 (GE Healthcare, Buckinghamshire, United Kingdom) for expression in bacteria as a glutathione *S*-transferase (GST) fusion protein and designated pCAGPM-HA-Caprin-1 and pGEX-GST-Caprin-1, respectively. The cDNAs of human G3BP1 and USP10 were also amplified from 293T cells by RT-PCR and cloned into pCAGPM-N-HA. The nucleotide residues of the adenine at 384, adenine at 385, cytosine at 387, and guanine at 388 of the JEV genome in pMWATG1 were replaced with guanine, cytosine, guanine, and cytosine, respectively, by PCR-based mutagenesis to change Lys^{97} and Arg^{98} of the core protein to Ala, yielding pMWAT/KR9798A. The cDNA of the mutant core protein was also cloned into pCAGPM-N-FLAG and pET21b. To generate stable cell lines expressing *Aequorea coerulescens* green fluorescent protein (AcGFP)-fused Caprin-1, the cDNA of human Caprin-1 was amplified by RT-PCR and cloned into pAcGFP N1 (Clontech, Mountain View, CA), and the Caprin-1-AcGFP gene was subcloned into the lentiviral vector pCSII-EF-RfA (21) and designated pCSII-EF-Caprin-1-AcGFP. All plasmids were confirmed by sequencing with an ABI Prism 3130 genetic analyzer (Applied Biosystems, Tokyo, Japan).

Cells and stress treatment. Mammalian cell lines, Vero (African green monkey kidney), 293T (human kidney), Huh7 (human hepatocellular carcinoma), and HeLa (human cervical carcinoma), were maintained in Dulbecco's modified Eagle's minimal essential medium (DMEM) (Sigma, St. Louis, MO) supplemented with 100 U/ml penicillin, 100 mg/ml streptomycin, nonessential amino acids (Sigma), and 10% fetal bovine serum (FBS). The mosquito cell line C6/36 (*Aedes albopictus*) was grown in Leibovitz's L-15 medium with 10% FBS. Huh7 cells were transduced with a lentiviral vector expressing Caprin-1-AcGFP and AcGFP and designated Huh7/Caprin-1-AcGFP and Huh7/AcGFP, respectively. For induction of SGs, cells were treated with sodium arsenite at a final concentration of 1.0 mM in the culture medium for 30 min prior to fixation or lysis of the cells. SG formation was defined morphologically by immunostaining using anti-SG-related factor antibodies described below. Cell viability was determined by using CellTiter-Glo (Promega, Madison, WI) according to the manufacturer's instruction.

Viruses. The wild-type and 9798A mutant of the JEV AT31 strain were generated by the transfection of pMWATG1 and pMWAT/KR9798A, respectively, as described previously (22). Viral infectivity was determined by an immunostaining focus assay as described previously (20), and the results are expressed in focus-forming units (FFU). JEV and DENV serotype 2 New Guinea C strain were amplified in C6/36 cells.

Antibodies. Anti-JEV core rabbit polyclonal antibody (PAb) and anti-JEV NS3 mouse monoclonal antibody (MAb) were prepared as described previously (20, 23). Anti-JEV NS2B rabbit PAb was generated with synthetic peptides of JEV NS2B at Scrum, Inc. (Tokyo, Japan). Anti-DENV core protein rabbit PAb was prepared by using a GST-fused recombinant protein containing amino acid residues 2 to 100 of the DENV core protein. Anti-FLAG mouse MAb (M2) and rabbit PAb and anti-β-actin mouse MAb were purchased from Sigma. Anti-hnRNP Q mouse MAb (ab10687), anti-USP10 rabbit PAb (ab70895), and anti-eIF4B rabbit PAb (ab78916) were purchased from Abcam (Cambridge, United Kingdom). Anti-eIF2α, anti-phospho-eIF2α, and anti-eIF3A rabbit PAbs were purchased from Cell Signaling Technology (Danvers, MA). Anti-HA mouse MAb (HA11), anti-HA rat MAb (3F10), anti-His mouse MAb, anti-GFP mouse MAb (JL-8), anti-JEV envelope protein mouse MAb (6B4A-10), anti-G3BP mouse MAb, anti-TIA-1 goat PAb, anti-Caprin-1 rabbit PAb, and anti-dsRNA mouse MAb were purchased from Covance (Richmond, CA), Roche (Mannheim, Germany), R&D Systems (Minneapolis, MN), Clontech, Chemicon (Temecula, CA), BD Biosciences (Franklin Lakes, NJ), Santa Cruz (Santa Cruz, CA), Proteintech (Chicago, IL), and Bio-

software (NIH, Bethesda, MD), and the relative levels for the indicated proteins are shown based on the level of the mock-infected cells. (D) Cellular localizations of G3BP, NS2B, and TIA-1 in Huh7 cells infected with JEV were determined at 24 h postinfection by immunofluorescence analysis with mouse anti-G3BP MAb, rabbit anti-NS2B PAb, and goat anti-TIA-1 PAb, followed by AF488-conjugated anti-mouse IgG, AF594-conjugated anti-rabbit IgG, and AF633-conjugated anti-goat IgG, respectively. Cell nuclei were stained with DAPI (gray). (E) Dynamics of G3BP and TIA-1 during JEV infection. Huh7 cells infected with JEV were immunostained at 0, 12, and 24 h postinfection (hpi) with mouse anti-G3BP MAb or goat anti-TIA-1 PAb and rabbit anti-NS2B PAb, followed by AF488-conjugated anti-mouse IgG or AF488-conjugated anti-goat IgG and AF594-conjugated anti-rabbit IgG, respectively. Cell nuclei were stained with DAPI (blue). (F) Cellular localization of SG-associated proteins (USP10, Caprin-1, TIA-1, hnRNP Q, eIF3A, and eIF4B) (green, AF488-conjugated secondary antibody) and JEV NS2B/NS3 (red, AF-594-conjugate secondary antibody) in Huh7 cells infected with JEV was determined by immunoblotting at 24 h postinfection. Cell nuclei were stained with DAPI (blue). (G) Numbers of G3BP-positive foci in 30 cells prepared as described in panel A were counted for each experimental condition. Lines, boxes, and error bars indicate the means, 25th to 75th percentiles, and 95th percentiles, respectively. The significance of differences between the means was determined by a Student's *t* test.*, $P < 0.01$; ND, no significant difference.

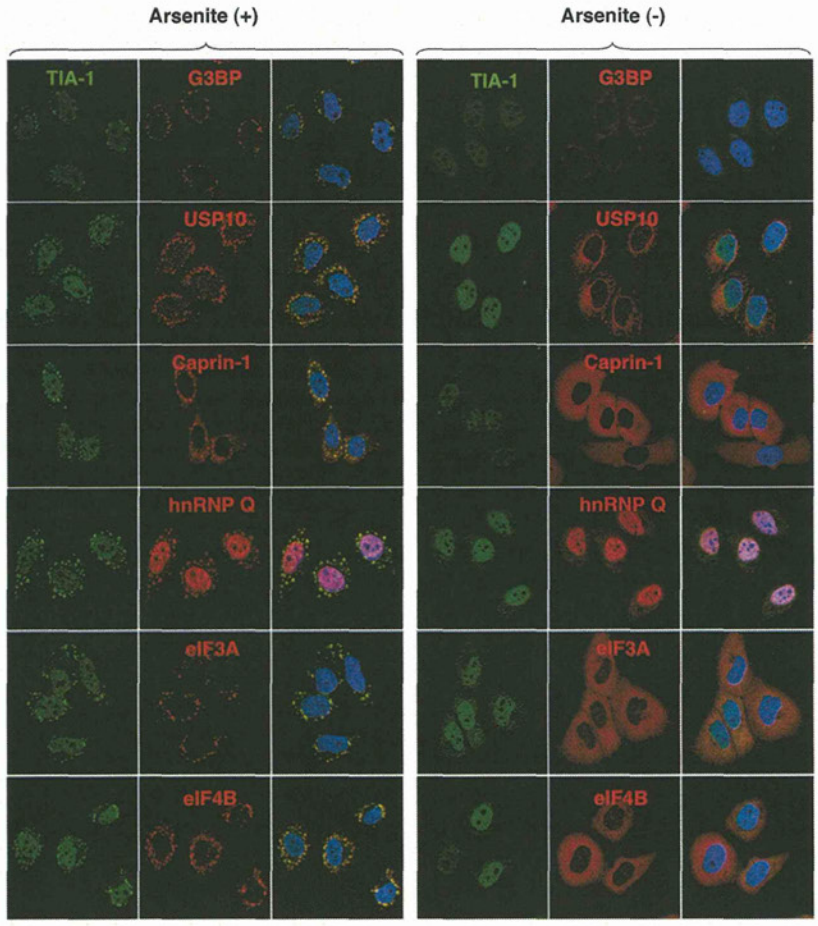

FIG 2 Each SG-associated factor forms SGs under oxidative stress. After treatment with 1.0 mM sodium arsenite for 30 min at 37°C, Huh7 cells were subjected to immunofluorescence analysis with the indicated primary antibodies, followed by AF488-conjugated anti-goat IgG and AF594-conjugated anti-mouse or rabbit IgG. Cell nuclei were stained with DAPI (blue).

center (Szirak, Hungary), respectively. Alexa Fluor (AF)-conjugated secondary antibodies were purchased from Invitrogen (Carlsbad, CA).

Immunofluorescence microscopy. Huh7 cells were fixed in 4% paraformaldehyde in phosphate-buffered saline (PBS) for 15 min at room temperature. After cells were quenched for 10 min with PBS containing 50 mM ammonium chloride (NH_4Cl), they were permeabilized with 0.2% Triton X-100 in PBS for 10 min and blocked with PBS containing 2% bovine serum albumin (BSA) for 30 min at room temperature. The cells were then incubated with the antibodies indicated in the figure legends. Nuclei were stained with 4′,6′-diamidino-2-phenylindole (DAPI). The samples were examined by a Fluoview FV1000 laser scanning confocal microscope (Olympus, Tokyo, Japan).

Transfection, immunoprecipitation, and immunoblotting. Plasmids were transfected into 293T or Huh7 cells by use of TransIT LT1 (Mirus, Madison, WI), and cells collected at 24 h posttransfection were subjected to immunostaining, immunoprecipitation, and/or immunoblotting as described previously (24). The immunoprecipitates were boiled in sodium dodecyl sulfate (SDS) sample buffer and subjected to SDS-polyacrylamide gel electrophoresis (SDS-PAGE). The proteins were transferred to polyvinylidene difluoride membranes (Millipore, Bedford, MA) and incubated with the appropriate antibodies. The immune complexes were visualized with SuperSignal West Femto substrate (Thermo Scientific, Rockford, IL) and detected by use of an LAS-3000 image analyzer system (Fujifilm, Tokyo, Japan).

FOS-tagged purification and mass spectrometry. pCAG-Core-FOS or empty vector was transfected into 293T cells, harvested at 24 h posttransfection, washed with cold PBS, suspended in cell lysis buffer (20 mM Tris-HCl, pH 7.4, 135 mM NaCl, 1% Triton X-100, and protease inhibitor cocktail [Complete; Roche]), and centrifuged at 14,000 × *g* for 20 min at 4°C. The supernatant was pulled down using 50 μl of STrEP-Tactin Sepharose (IBA, Gottingen, Germany) equilibrated with cell lysis buffer for 2 h at 4°C. The affinity beads were washed three times with cell lysis buffer and suspended in 2× SDS-PAGE sample buffer. The proteins were subjected to SDS-PAGE, followed by Coomassie brilliant blue (CBB) staining using CBB Stain One (Nakalai Tesque, Kyoto, Japan). The gels were divided into 10 pieces, and each fraction was trypsinized and subjected to liquid chromatography-tandem mass spectrometry (LC-MS/MS) analysis to identify coimmunoprecipitated proteins. All of the proteins in gels were identified comprehensively, and the proteins detected in cells transfected with pCAG-Core-FOS but not in those with empty vector were regarded as candidates for binding partners of JEV core.

Gene silencing. A commercially available small interfering RNA (siRNA) pool targeting Caprin-1 (siGENOME SMARTpool, human Caprin1) and control nontargeting siRNA were purchased from Dharmacon (Buckinghamshire, United Kingdom) and transfected into 293T cells using Lipofectamine RNAiMAX (Invitrogen) according to the manufacturer's protocol.

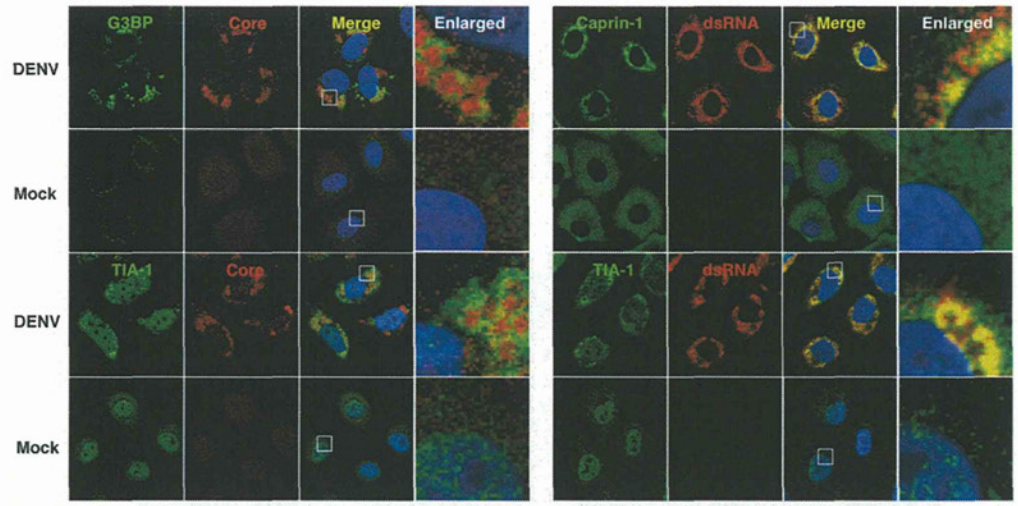

FIG 3 Subcellular localizations of the SG-associated proteins during DENV infection. Cellular localizations of G3BP, Caprin-1, and TIA-1 (green, AF488-conjugated secondary antibody) and viral components (core protein and dsRNA) (red, AF-594-conjugate secondary antibody) in Huh7 cells infected with DENV were determined by immunofluorescence analysis using the appropriate antibodies at 48 h postinfection. Cell nuclei were stained with DAPI (blue).

Preparation of recombinant proteins and GST pulldown assay. His-tagged JEV core protein (core-His) was purified as described in a previous report (25). Briefly, core-His was expressed in *Escherichia coli* (*E. coli*) Rosetta-gami 2(DE3) strain cells (Novagen-Merck) transformed with pET21b-Core-His (WT or 9798A). Bacteria grown to an optical density at 600 nm of 0.6 were induced with 0.5 mM isopropyl-β-D-thiogalactopyranoside (IPTG), incubated for 5 h at 37°C with shaking, collected by centrifugation at 6,000 × *g* for 10 min, lysed in 10 ml of bacteria lysis buffer (50 mM Tris-HCl, pH 7.4, 150 mM NaCl, 1 mM EDTA, 1% Triton X-100, and protease inhibitor cocktail [Complete; Roche]) by sonication on ice, and centrifuged at 10,000 × *g* for 15 min. The supernatant containing core-His was subjected to ammonium sulfate fractionation, followed by cation exchange chromatography with a HiTrap SP column (GE Healthcare). The eluted core-His recombinant protein was dialyzed with 50 mM Tris-HCl buffer containing 150 mM NaCl at 4°C overnight. GST-fused Caprin-1 (GST-Caprin-1) was expressed in *E. coli* BL21(DE3) cells transformed with pGEX-GST-Caprin-1. Bacteria grown to an optical density at 600 nm of 1.0 were induced with 0.1 mM IPTG, incubated for 5 h at 25°C with shaking, collected by centrifugation at 6,000 × *g* for 10 min, lysed in 10 ml of bacteria lysis buffer by sonication on ice, and centrifuged at 10,000 × *g* for 15 min. The supernatant was mixed with 200 μl of glutathione-Sepharose 4B beads (GE Healthcare) equilibrated with bacteria lysis buffer for 1 h at room temperature, and then the beads were washed five times with lysis buffer. Twenty micrograms of GST-Caprin-1 or GST was mixed with equal volumes of the purified core-His for 2 h at 4°C with gentle agitation. The beads were washed five times with bacteria lysis buffer and then suspended in SDS-PAGE sample buffer.

Mouse experiments. Experimental infections were approved by the Committee for Animal Experiment of RIMD, Osaka University (H19-2-0). Female ICR mice (3 weeks old) were purchased from CLEA Japan (Tokyo, Japan) and kept in specific pathogen-free environments. Groups of mice ($n = 10$) were intraperitoneally inoculated with 5×10^4 FFU (100 μl) of the viruses. The mice were observed for 3 weeks after inoculation to determine survival rates. To examine viral growth in the brain, 5×10^4 FFU of the viruses were intraperitoneally administered to the groups of mice ($n = 3$). At 7 days postinfection, mice were euthanized, and the cerebrums were collected. The infectious titers in the homogenates of the cerebrums were determined in Vero cells as described above.

RESULTS

JEV infection confers resistance to SG induction. To examine the formation of SGs in cells infected with JEV, Huh7 cells were infected with JEV at a multiplicity of infection (MOI) of 0.5, and the expression of JEV proteins and an accepted marker for SGs, G3BP, was determined by immunofluorescence analysis at 24 h postinfection. G3BP was mainly accumulated in the perinuclear region and partially colocalized with the JEV core protein, while only partial colocalization with the NS2B protein was also observed (Fig. 1A, left). In addition, a few small G3BP-positive foci were scattered in the cytoplasm. This accumulation of G3BP was observed in not only Huh7 cells but also other cell lines, i.e., 293T and HeLa cells, infected with JEV (Fig. 1B). However, the expression level of G3BP in cells infected with JEV was comparable to that in mock-infected cells (Fig. 1C). To further investigate SG induction by JEV infection, expression of TIA-1, another SG marker, was examined. Although accumulation of TIA-1 in the perinuclear region was not observed, a few TIA-1-positive foci were observed in the JEV-infected cells and were colocalized with G3BP and JEV NS2B, indicating that SG foci were induced in cells infected with JEV (Fig. 1D). The accumulation of G3BP and the aggregation of TIA-1, indicating SG formation, appeared at 24 h postinfection in accord with the expression of viral proteins (Fig. 1E). We further examined the dynamics of other SG-associated factors in cells infected with JEV. Each factor formed clear SGs in cells treated with sodium arsenite, a potent SG inducer eliciting oxidative stress (Fig. 2). As shown in Fig. 1F, three distinct patterns of the subcellular localization of SG components were observed. USP10 and Caprin-1 were accumulated in the perinuclear region and also formed a few small foci scattered throughout the cytoplasm, as seen for G3BP; TIA-1 and hnRNP Q formed cytoplasmic foci but were not accumulated in the perinuclear region; and subcellular localization of eIF3A and eIF4B was not changed. The cytoplasmic foci were confirmed as SGs by immunofluorescence analyses using specific antibodies to SG-associated factors (data not shown). Taken together, these results indicate that JEV infection induces accumulation of several RBPs and formation of a few SGs.

It has been shown previously that infection with WNV or DENV confers resistance to SG formation induced by sodium arsenite (15). To determine the effect of JEV infection on the SG

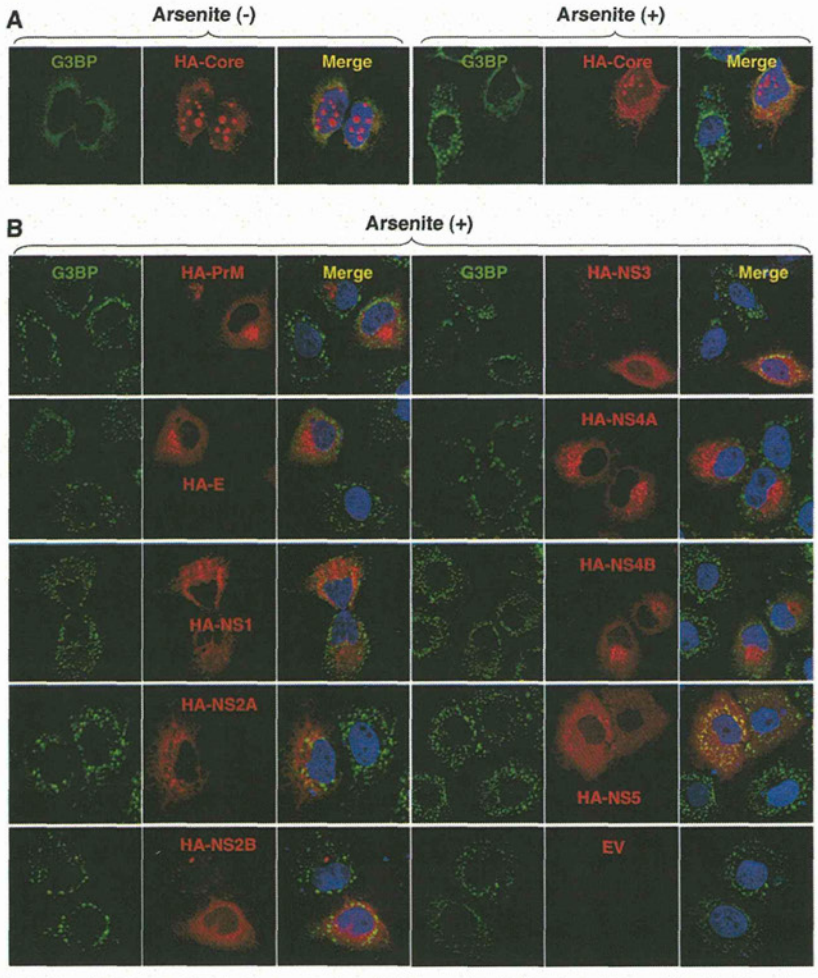

FIG 4 Inhibition of the arsenite-induced SG formation by the expression of JEV proteins. (A) Huh7 cells transfected with a plasmid, pCAGPM-HA-Core, were treated with or without 1.0 mM sodium arsenite for 30 min at 37°C, and the cellular localizations of G3BP and HA-Core were determined at 24 h posttransfection by immunofluorescence analysis with mouse anti-G3BP MAb and rat anti-HA MAb, followed by AF488-conjugated anti-mouse IgG and AF594-conjugated anti-rat IgG, respectively. Cell nuclei were stained with DAPI (blue). (B) Huh7 cells, which were separately transfected with a plasmid expressing an individual viral protein (pCAGPM-HA-JEV protein) as indicated in the figure, were treated with 1.0 mM sodium arsenite for 30 min at 37°C and subjected to an immunofluorescence assay using mouse anti-G3BP MAb and rat anti-HA MAb, followed by AF488-conjugated anti-mouse IgG and AF594-conjugated anti-rat IgG, respectively. Cell nuclei were stained with DAPI (blue).

formation induced by sodium arsenite, JEV-infected cells were treated with 0.5 mM sodium arsenite for 30 min at 24 h postinfection. Although many G3BP-positive foci were observed in mock-infected cells by the treatment with sodium arsenite, accumulation of G3BP in the perinuclear region was observed in the JEV-infected cells (Fig. 1A, right), and the numbers of G3BP-positive foci in the JEV-infected cells were less than those in the mock-infected cells (Fig. 1G). Although it has been reported that a significant reduction of the phosphorylation at Ser^{51} of eIF2α in cells treated with arsenite was induced by infection with WNV (15), the phosphorylation of eIF2α was slightly suppressed in the JEV-infected cells (Fig. 1C). Furthermore, while previous studies reported that Caprin-1 and TIA-1 were colocalized with dsRNA in cells infected with DENV (15, 26), no colocalization of G3BP or TIA-1 with the DENV core protein was observed in the present study (Fig. 3), suggesting that the mechanisms of the viral circumvention of SG formation in cells infected with JEV are different from those in cells infected with WNV and DENV.

JEV core protein suppresses SG formation induced by sodium arsenite. To elucidate the molecular mechanisms of suppression of SG formation induced by sodium arsenite during JEV infection, we tried to identify which viral protein(s) is responsible for the SG inhibition. Since G3BP was colocalized with JEV core protein, we first examined the involvement of the core protein in the perinuclear accumulation of G3BP and in the suppression of SG formation. The expression of JEV core protein alone induced the accumulation of G3BP in the perinuclear region (Fig. 4A, left panel) and suppressed sodium arsenite-induced SG formation (Fig. 4A, upper right cell in the right panel), similarly to JEV infection. In contrast, inhibition of SG formation induced by sodium arsenite was not observed in cells expressing other JEV proteins (Fig. 4B). These results suggest that JEV core protein is responsible for the circumvention of the SG formation observed in cells infected with JEV.

JEV core protein directly interacts with Caprin-1, an SG-associated cellular factor. Since JEV core protein was suggested to

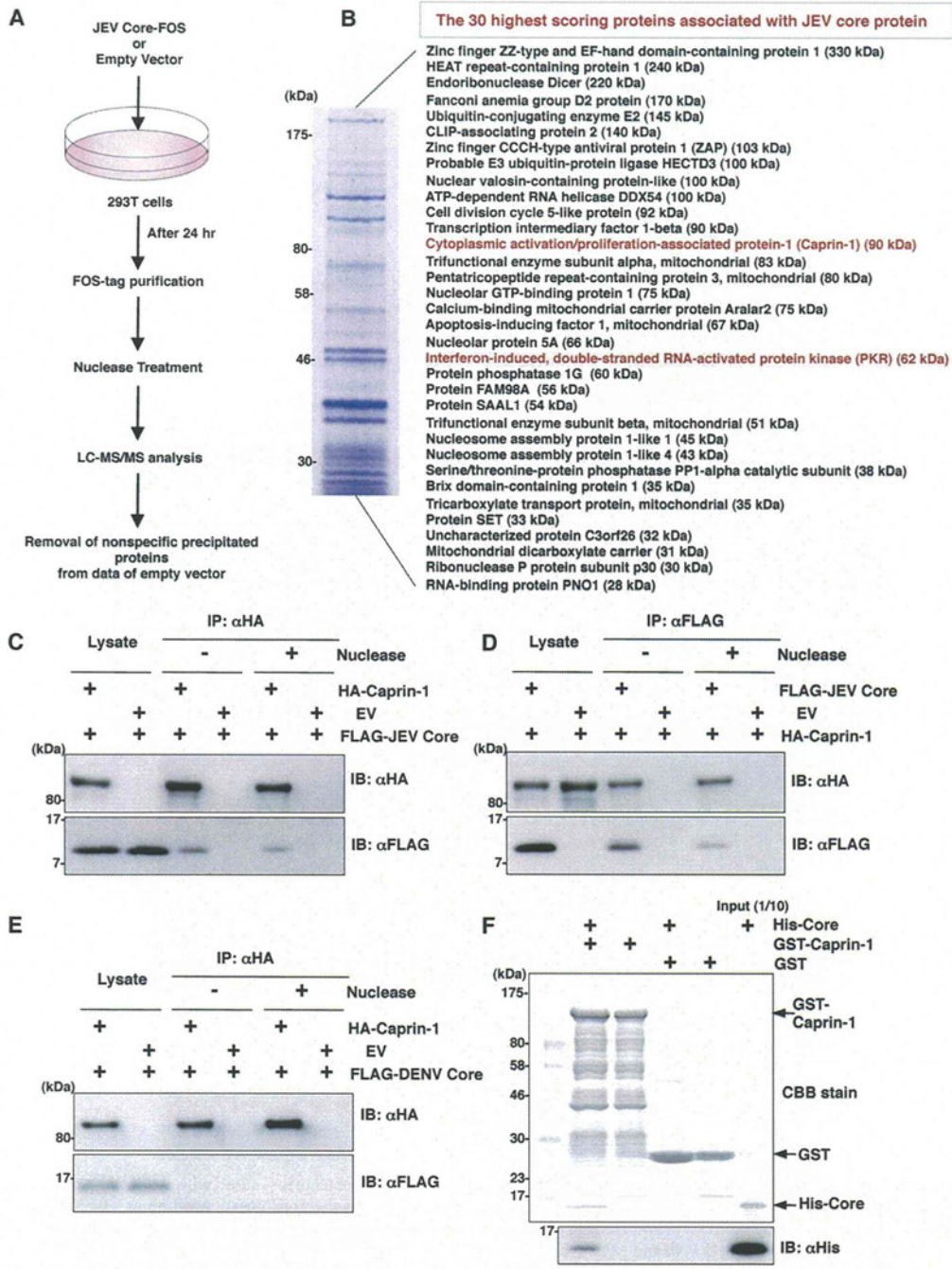

FIG 5 JEV core protein directly interacts with Caprin-1, an SG-associated cellular factor. (A) Identification of host cellular proteins associated with JEV core protein by FOS-tagged purification and LC-MS/MS analysis. Overview of the FOS-tagged purification of cellular proteins associated with JEV core protein. (B) The 30 candidate proteins as binding partners of JEV core protein exhibiting high scores are listed. PKR and Caprin-1 are indicated in red. (C and D) FLAG-JEV core protein and HA-Caprin-1 were coexpressed in 293T cells, and the cell lysates harvested at 24 h posttransfection were treated with or without micrococcal nuclease for 30 min at 37°C and immunoprecipitated (IP) with anti-HA (αHA) or anti-FLAG (αFLAG) antibody, as indicated. The precipitates were subjected to immunoblotting (IB) to detect coprecipitated counterparts. (E) FLAG-DENV core protein was coexpressed with HA-Caprin-1 in 293T cells, immunoprecipitated with anti-HA antibody, and immunoblotted with anti-HA or anti-FLAG antibody. (F) His-tagged JEV core protein was incubated with either GST-fused Caprin-1 or GST for 2 h at 4°C, and the precipitates obtained by GST pulldown assay were subjected to CBB staining and immunoblotting with anti-His antibody.

participate in the inhibition of SG formation, we tried to identify cellular factors associated with the core protein by LC-MS/MS analysis, as shown in Fig. 5A. Among the 30 factors with the best scores, two SG-associated proteins, PKR (Mascot search score, 206) and Caprin-1 (Mascot search score, 153), were identified as binding partners of JEV core protein (Fig. 5B). Although PABP1, hnRNP Q, Staufen, G3BP, and eIF4G were also identified, their scores were lower than those of PKR and Caprin-1. Because the

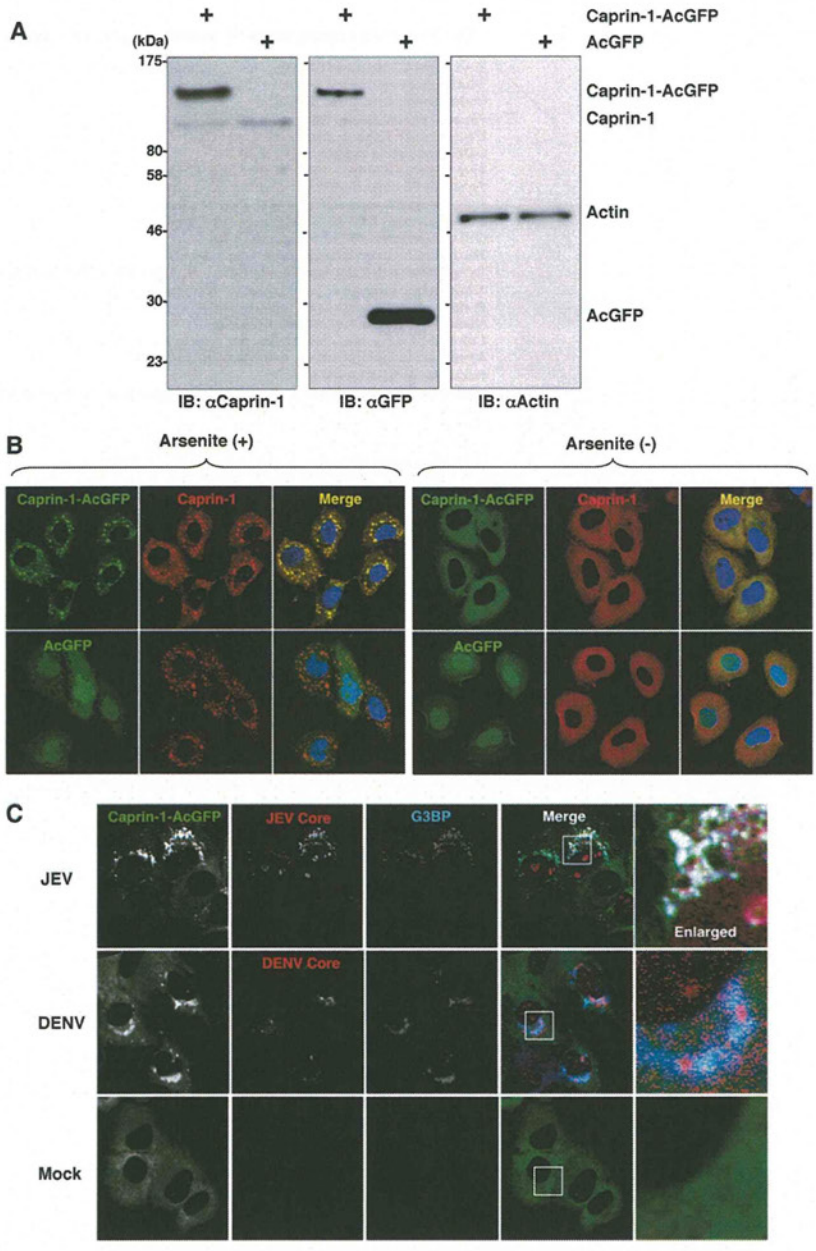

FIG 6 Caprin-1 is colocalized with the JEV core protein in the perinuclear region. (A) Expression of Caprin-1 fused with AcGFP (Caprin-1-AcGFP), Caprin-1, actin, or AcGFP in lentivirally transduced Huh7 cells was determined by immunoblotting using the appropriate antibodies. (B) Subcellular localization of Caprin-1-AcGFP or AcGFP (green) and endogenous Caprin-1 (red) in cells treated with/without 1.0 mM sodium arsenite for 30 min at 37°C was determined by immunofluorescence assay with rabbit anti-Caprin-1 PAb and AF594-conjugated anti-rabbit IgG. Cell nuclei were stained with DAPI (blue). (C) Huh7/Caprin-1-AcGFP cells were infected with either JEV or DENV at an MOI of 0.5, and the cellular localizations of JEV and DENV core (red) with Caprin-1-AcGFP and G3BP (blue) were determined at 24 h and 48 h postinfection, respectively. Cells were stained with mouse anti-G3BP MAb and rabbit anti-JEV or DENV core protein PAb, followed by AF633-conjugated anti-mouse IgG and AF594-conjugated anti-rabbit IgG, respectively, and examined by immunofluorescence analysis.

results shown in Fig. 1B suggest that the inhibition of SG formation takes place downstream of eIF2α phosphorylation, we focused on Caprin-1 as a key factor involved in the inhibition of SG formation in cells infected with JEV. To confirm the specific interaction of JEV core protein with Caprin-1, FLAG-JEV core protein and HA-Caprin-1 were coexpressed and immunoprecipitated with anti-HA or anti-FLAG antibody in the presence or absence of nuclease. FLAG-JEV core protein was coprecipitated with HA-Caprin-1 irrespective of nuclease treatment (Fig. 5C and D), suggesting that the interaction between JEV core protein and Caprin-1 is a protein-protein interaction. On the other hand, FLAG-DENV core protein was not coprecipitated with HA-Caprin-1 (Fig. 5E), indicating that the interaction with Caprin-1 was specific for JEV core protein. Next, the direct interaction be-

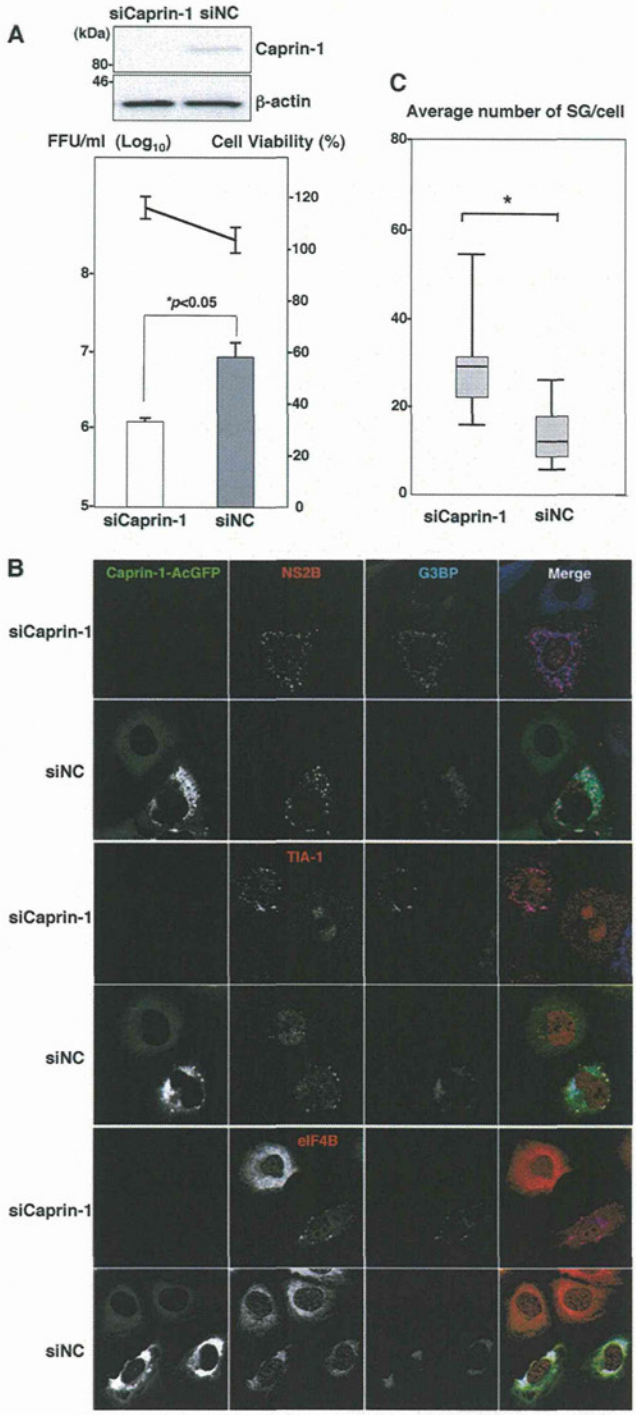

FIG 7 Knockdown of Caprin-1 cancels SG inhibition during JEV infection and suppresses viral propagation. (A) (Upper) The levels of expression of Caprin-1 in cells transfected with either siCaprin-1 or siNC was determined by immunoblotting using anti-Caprin-1 and anti-β-actin antibodies at 72 h posttransfection (top panel). At 48 h posttransfection with either siCaprin-1 or siNC, Huh7/Caprin-1-AcGFP cells were inoculated with JEV at an MOI of 0.5. At 24 h postinfection (72 h posttransfection), the infectious titers in the supernatants were determined by focus-forming assay in Vero cells (bottom panel, bar graph). Cell viability was determined at 72 h posttransfection and calculated as a percentage of the viability of cells treated with siNC (bottom panel, line graph). The results shown are from three independent assays, with the error bars representing the standard deviations. (B) At 48 h posttransfection with either siCaprin-1 or siNC, Huh7/Caprin-1-AcGFP cells were inoculated with JEV at an MOI of 0.5. The cellular localizations of SG-associated factors and JEV NS2B were determined at 24 h postinfection (72 h posttransfection) by immunofluorescence analysis with mouse anti-G3BP MAb and rabbit anti-NS2B PAb, rabbit anti-eIF4B PAb, or goat anti-TIA-1 PAb, followed by AF633-conjugated anti-mouse IgG and AF594-conjugated anti-rabbit IgG or AF594-conjugated anti-goat IgG, respectively. (C) Numbers of G3BP-positive foci in 30 cells prepared as described in panel B were counted. Lines, boxes, and error bars indicate the means, 25th to 75th percentiles, and 95th percentiles, respectively. The significance of differences between the means was determined by a Student's *t* test. *, $P < 0.01$.

tween JEV core protein and Caprin-1 was examined by a GST-pulldown assay using purified proteins expressed in bacteria. The His-tagged core protein was coprecipitated with GST-tagged Caprin-1, suggesting that JEV core protein directly interacts with Caprin-1 (Fig. 5F).

To further determine the cellular localization of Caprin-1 in JEV-infected cells, Caprin-1 fused with AcGFP (Caprin-1-AcGFP) was lentivirally expressed in Huh7 cells. The levels of expression and recruitment of Caprin-1-AcGFP into SGs were determined by immunoblotting and immunofluorescence analysis, respectively (Fig. 6A and B). In cells infected with JEV, Caprin-1-AcGFP was concentrated in the perinuclear region and colocalized with core protein and G3BP, while no colocalization of the proteins was observed in cells infected with DENV (Fig. 6C), suggesting that Caprin-1 directly interacts with JEV core protein in the perinuclear region of the infected cells.

Knockdown of Caprin-1 cancels SG inhibition during JEV infection and suppresses viral propagation. To assess the biological significance of the interaction of JEV core protein with Caprin-1 in JEV propagation, the expression of Caprin-1 was suppressed by using Caprin-1-specific siRNAs (siCaprin-1). Transfection of siCaprin-1 efficiently and specifically knocked down the expression of Caprin-1 with a slight increase of cell viability and decreased the production of infectious particles in the culture supernatants of cells infected with JEV, in comparison with those treated with a control siRNA (siNC) (Fig. 7A). Furthermore, immunofluorescence analyses revealed that knockdown of Caprin-1 increased the number of G3BP-positive granules colocalized with SG-associated factors, including TIA-1 and eIF4B, and inhibited the G3BP concentration in the perinuclear region (Fig. 7B and C). These results suggest that knockdown of Caprin-1 suppresses JEV propagation through the induction of SG formation.

Lys^{97} and Arg^{98} in the JEV core protein are crucial residues for the interaction with Caprin-1. To determine amino acid residues of the core protein that are required for the interaction with Caprin-1, we constructed a putative model based on the structural information of the DENV core protein previously resolved by nuclear magnetic resonance (NMR) (27), as shown in Fig. 8A. Based on this model, we selected hydrophobic amino acids, which were located on the solvent-exposed side in the α1 and α4 helices, as amino acid residues responsible for the binding to host proteins. Amino acid substitutions in each of the α-helices shown in Fig. 8B were designed in the context of FLAG-Core (Mα1 and Mα4), and the interaction of FLAG-Core mutants with Caprin-1 was examined by immunoprecipitation analysis. WT and Mα1, but not Mα4, core proteins were immunoprecipitated with Caprin-1 (Fig. 8B). To determine the amino acids responsible for interaction with Caprin-1, further alanine substitutions were introduced in the α4 helix, and the interaction was examined by immunopre-

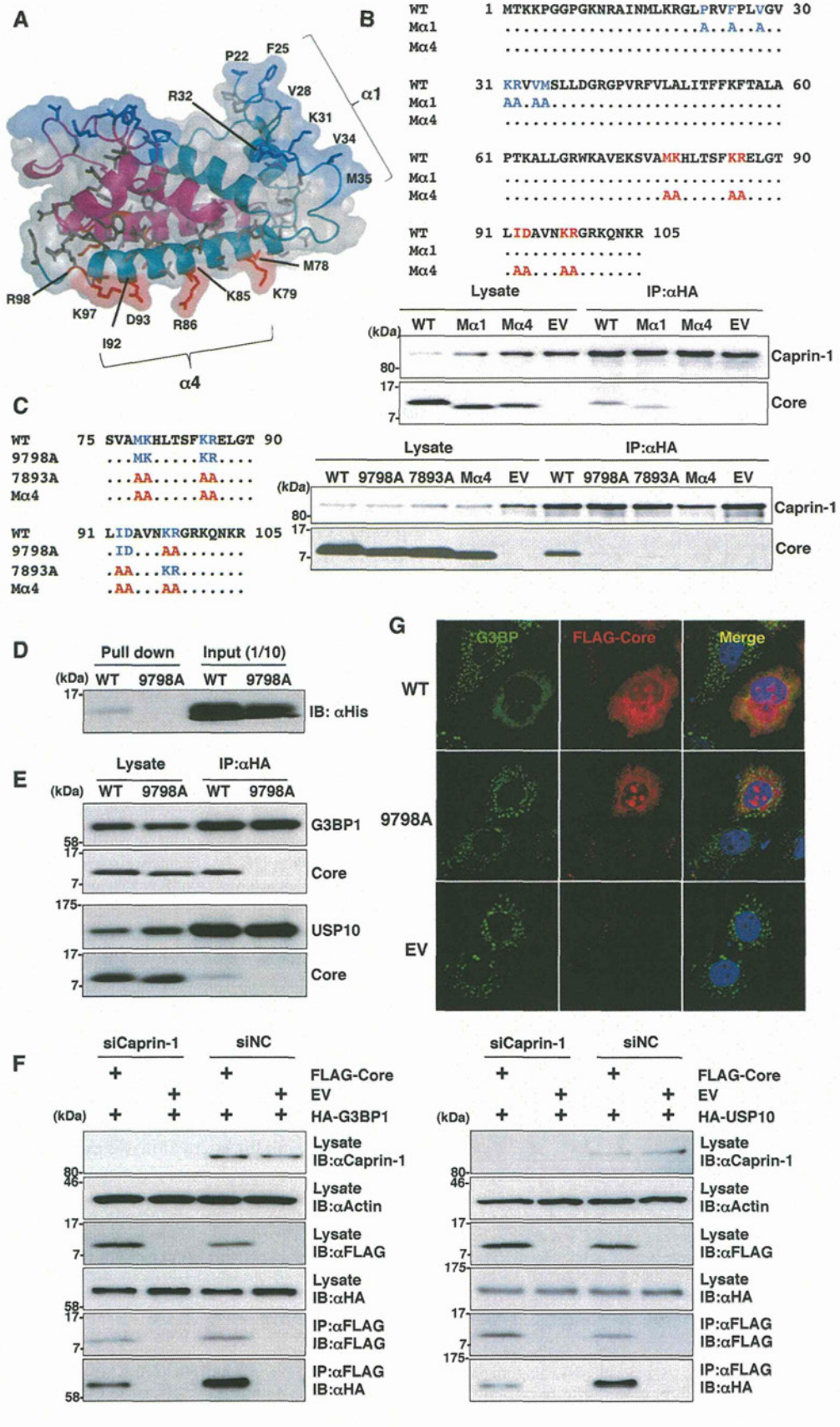

cipitation assay. As shown in Fig. 8C, double replacing both Lys^{97} and Arg^{98} with Ala (9798A) completely abrogated the interaction with Caprin-1. The importance of these two amino acids in the interaction with Caprin-1 was also confirmed by GST pulldown assay (Fig. 8D). These results indicate that Lys^{97} and Arg^{98} in the JEV core protein are crucial for the interaction with Caprin-1. Since G3BP has been reported to be one of the key molecules for SG formation and interacts with several SG component molecules including Caprin-1 and USP10 (28, 29), interactions of the core protein with SG components were examined by immunoprecipitation assay. The wild-type but not mutant 9798A core protein was associated with G3BP1 and USP10 (Fig. 8E). In addition, the knockdown of Caprin-1 weakened the interactions of core protein with G3BP1 or USP10 (Fig. 8F). These findings indicate that JEV core protein associates with several SG component molecules, such as G3BP1 and USP10, through the interaction with Caprin-1. Next, the role of the interaction between JEV core protein and Caprin-1 in the suppression of SG formation was examined by immunofluorescence analysis. Although the expression of the wild-type JEV core protein suppressed the SG formation induced by sodium arsenite treatment, as shown above, expression of the 9798A mutant did not (Fig. 8G), suggesting that the interaction of JEV core protein with Caprin-1 through Lys^{97} and Arg^{98} plays a crucial role in the inhibition of SG formation.

Interaction of the JEV core protein with Caprin-1 plays crucial roles not only in viral propagation *in vitro* but also in the pathogenesis in mice through the suppression of SG formation. To further examine the biological significance of the interaction between the JEV core protein and Caprin-1 in viral replication, we generated a mutant infectious cDNA clone (pMWJEAT/9798AA) of JEV encoding a mutant core protein deficient in the binding to Caprin-1 based on pMWJEAT. First, the cellular localization of the core protein in the 9798A mutant JEV-infected cells was examined by immunofluorescence analysis. The 9798A mutant core protein, as well as the wild-type core protein, was localized in the nucleus and the perinuclear region (Fig. 9A). However, the 9798A mutant core protein was not colocalized with Caprin-1, in contrast to the wild-type core protein. The sizes of infectious foci in Vero cells infected with the 9798A mutant were significantly smaller than those infected with the wild-type JEV (Fig. 9B). Furthermore, the infectious titers in C6/36 and Vero cells infected with the 9798A mutant were 6.1- and 12.6-fold lower than those infected with wild-type JEV at 48 h postinfection, respectively (Fig. 9C), suggesting that interaction of the JEV core protein with Caprin-1 plays crucial roles in the propagation of JEV in both insect and mammalian cells. Cells infected with the 9798A mutant induced SGs containing both G3BP and Caprin-1, in contrast to the accumulation of G3BP in the perinuclear region observed in those infected with the wild-type JEV (Fig. 9D). The numbers of foci in cells infected with the 9798A mutant were higher than those in cells infected with the wild-type JEV (Fig. 9E), indicating that the interaction of the JEV core protein with Caprin-1 is crucial for the suppression of SG formation. Finally, we examined the biological relevance of the interaction of JEV core protein with Caprin-1 in viral replication *in vivo*. Infectious particles were recovered from the cerebrums of ICR mice inoculated with wild-type JEV but not from those inoculated with the 9798A mutant (Fig. 9F). In addition, all 10 mice had died by 12 days postinoculation with the wild-type JEV, while only 1 mouse had died at day 10 postinoculation with the 9798A mutant (Fig. 9G). Collectively, these results suggest that the interaction of JEV core protein with Caprin-1 plays crucial roles not only in viral replication *in vitro* but also in pathogenesis in mice through the suppression of SG formation.

DISCUSSION

Viruses are obligatory intracellular parasites, and their life cycles rely on host cellular functions. Many viruses have evolved to inhibit SG formation and thereby evade the host translation shutoff mechanism and facilitate viral replication (6, 30), while some viruses co-opt molecules regulating SG formation for viral replication (11, 31). The vaccinia virus subverts SG components to generate aggregates containing G3BP, Caprin-1, eIF4G, eIF4E, and mRNA of the virus, but not of the host, in order to stimulate viral translation (11). Replication, translation, and assembly of transmissible gastroenteritis coronavirus, a member of the *Coronaviridae* family, are regulated by the interaction of polypyrimidine tract-binding protein and TIA-1 with viral RNA (31). HIV-1 utilizes Staufen1, which is a principal component of SG, in the viral RNA selection to form ribonucleoproteins (RNPs) through interaction with Gag protein, instead of SG translation silencing (8). In the case of flaviviruses, TIA-1 and TIAR bind to the 3′ untranslated region (UTR) of the negative-stranded RNA of WNV to facilitate viral replication (16), and G3BP1, Caprin-1, and USP10 interact with DENV RNA, although the biological significance of these interactions remains unknown (26). In this study, we have shown that JEV infection suppresses SG formation by the recruitment of several effector molecules promoting SG assembly, including G3BP and USP10, to the perinuclear region through the interaction of JEV core protein with Caprin-1. Furthermore, a mutant JEV carrying a core protein incapable of binding to

FIG 8 Lys^{97} and Arg^{98} in the JEV core protein are crucial residues for the interaction with Caprin-1. (A) Putative structural model of the core protein homodimer of JEV deduced from that of DENV obtained from the Protein Data Bank (accession number 1R6R) by using PyMOL software. The two α helices (α1 and α4) are indicated. (B) FLAG-Core mutants in which the hydrophobic amino acid residues in the α1 helix (Mα1) or α4 helix (Mα4) were replaced with alanine were coexpressed with HA-Caprin-1 in 293T cells, immunoprecipitated (IP) with anti-HA antibody, and examined by immunoblotting (IB) with anti-HA or anti-FLAG antibody. (C) FLAG-Core mutants in which the Met^{78}, Lys^{79}, Lys^{85}, Arg^{86}, Ile^{92}, and Asp^{93} (7893A) or Lys^{97} and Arg^{98} (9798A) in the α4 helix domain were replaced with alanine were coexpressed with HA-Caprin-1 in 293T cells and examined as described in panel B. (D) The His-tagged JEV core protein (WT or 9798A) was incubated with GST-fused Caprin-1 for 2 h at 4°C, and the precipitates obtained by GST pulldown assay were subjected to immunoblotting with anti-His antibody. (E) FLAG-Core (WT or 9798A) was coexpressed with HA-G3BP1 or HA-USP10 in 293T cells, immunoprecipitated with anti-HA antibody, and immunoblotted with anti-HA and anti-FLAG antibodies. (F) FLAG-JEV Core was coexpressed with HA-G3BP1 or HA-USP10 in 293T cells transfected with either siCaprin-1 or siNC at 72 h posttransfection, immunoprecipitated with anti-FLAG antibody, and immunoblotted with anti-HA and anti-FLAG antibodies. The cell lysates were also subjected to immunoblotting with anti-Caprin-1 and anti-β-actin antibodies to evaluate the knockdown efficiency of Caprin-1. (G) The cellular localizations of G3BP and FLAG-Core (WT or 9798A) were determined at 24 h posttransfection after treatment with 1.0 mM sodium arsenite for 30 min at 37°C by immunofluorescence analysis with mouse anti-G3BP MAb and rabbit anti-FLAG PAb, followed by AF488-conjugated anti-mouse IgG and AF594-conjugated anti-rabbit IgG, respectively. Cell nuclei were stained with DAPI (blue).